Reinterpretation of velocity-dependent atomic friction: Influence of the inherent instrumental noise in friction force microscopes

Yalin Dong,[1,*] Hongyu Gao,[2,†] Ashlie Martini,[2,‡] and Philip Egberts[3,§]

[1]*Department of Mechanical Engineering, University of Akron, 302 Buchtel Common, Akron, Ohio 44325, USA*
[2]*School of Engineering, University of California Merced, 5200 North Lake Road, Merced, California 95343, USA*
[3]*Department of Mechanical and Manufacturing Engineering, University of Calgary, 40 Research Place NW,
Calgary, Alberta T2L 1Y6, Canada*

We have applied both the master equation method and harmonic transition state theory to interpret the velocity-dependent friction behavior observed in atomic friction experiments. To understand the discrepancy between attempt frequencies measured in atomic force microscopy experiments and those estimated by theoretical models, both thermal noise and instrumental noise are introduced into the model. It is found that the experimentally observed low attempt frequency and the transition point at low velocity regimes can be interpreted in terms of the instrumental noise inherent in atomic force microscopy. In contrast to previous models, this model also predicts (1) the existence of a two-slope curve of velocity dependence and (2) the decrease of critical velocity with temperature, which provides clues for further experimental verification of the influence of instrumental noise in friction measurements.

PACS number(s): 05.40.Ca, 68.35.Af, 68.37.Ps, 81.40.Pq

I. INTRODUCTION

With the advent of atomic force microscopy (AFM) [1], it became possible to measure friction at the atomic length scale in single asperity contacts [2]. These atomic-scale friction measurements showed many deviations from the well-known friction laws observed at the macroscale. One example of such a deviation is that friction varies with AFM tip velocity or sliding speed [3,4], often termed velocity-dependent atomic friction. Recently, there has been great interest and significant progress in understanding this phenomenon, which manifests itself as increasing friction with increased sliding speeds and decreased temperatures. In the pioneering AFM experiments conducted by Gnecco *et al.* [4], a logarithmic velocity dependence of friction was observed, which was then rationalized in terms of thermal activation [4–7]. With the assistance of thermal energy, a single asperity AFM tip can jump between atomic lattice sites at lower lateral forces than in the absence of thermal energy, leading to a reduction in friction. The dependence of friction on sliding speed results from the shorter time that is allowed for thermal energy to assist the tip in reaching the next atomic lattice position. As a result, the friction F logarithmically increases with the sliding velocity v according to the relation below:

$$F = F_c - \left| \beta k_B T \ln \left(\frac{v_c}{v} \right) \right|^{2/3},\tag{1}$$

where F_c is the maximum friction at $T = 0$, v_c is the critical velocity at which the friction reaches F_c and does not increase further as v increases, and β is a parameter determined by the shape of the corrugation potential. The parameter v_c can be determined by $v_c = (2 f_0 \beta T)/(3 k_{\text{eff}} \sqrt{F_c})$, where f_0 is the

attempt frequency and k_{eff} is the effective spring constant of the AFM cantilever, tip, and sample contact, or the slope of the lateral force measured while the tip is stuck at a single lattice site. Equation (1) has been widely used to interpret AFM experimental data [5,6,8–11].

Despite the great success in interpreting atomic friction data through the thermal activation mechanism and its wide applicability in fitting AFM experimental data, significant discrepancies in terms of the calculated attempt frequencies have existed between various experiments, but perhaps more importantly between experiment and theory [12]. The attempt frequency for thermal activation is the characteristic frequency with which the tip apex in contact with the surface oscillates as a result of thermal energy. The magnitude of the attempt frequency depends on the effective mass of the tip involved in thermal activation. It has been theoretically revealed that the mass of the tip apex is on the order of $m = 10^{-20}$ kg or lighter [13–19]. Therefore, from the perspective of theory, the magnitude of the attempt frequency would be on the order of GHz or even THz. However, the reported attempt frequencies obtained from fitting AFM friction data as a function of sliding speed consistently fall out of the range of theoretical predictions and vary widely. For example, the following attempt frequencies have been measured in AFM experiments: 6 MHz on NaCl(100) surfaces [4,5], 13–53 kHz on mica surfaces under different normal loads [6], 24 MHz on surfaces of highly oriented pyrolytic graphite [9], and 49 kHz on Au(111) surfaces [11]. All of these experimentally determined frequencies are much smaller than those predicted by theoretical approaches and cannot be explained within the framework of thermal activation.

In this work, we will re-examine this discrepancy by accounting for the additional mechanical energy resulting from instrumental noise inherent in AFM measurements. This instrumental noise, although being often neglected once a successful measurement has been achieved, will be shown to have significant influence on the measured velocity-dependent friction behavior. Examples explicitly showing the influence

---

*ydong@uakron.edu
†hgao2@ucmerced.edu
‡amartini@ucmerced.edu
§philip.egberts@ucalgary.ca

of mechanical vibrations include the formation of unstable tip-sample contacts [20] and can result in unintended oscillations of the cantilever (also possibly resulting in an unstable tip-sample contact) [21], a transition to the low friction regime of dynamic superlubricity [22], and a significant reduction in wear of AFM probes [23]. Similar to thermal noise, mechanical noise can suppress atomic friction through activating motion at the contact [6,24,25]. However, in almost all conventional models of atomic friction, instrumental noise is rarely considered, and its effect on the velocity dependence of atomic friction remains unexplored. We here restrict our definition of instrumental noise to displacement noise as it is one of the the primary noise sources to modulate the contact formed between the tip and the surface [25,26]. In this work, we will start from the theoretical model, the Prandtl-Tomlinson (PT) model [27,28], and then investigate the effect of the instrumental noise inherent in AFM through the master equation method and harmonic transition state theory (HTST). The attempt frequency discrepancy between experiments and simulations will be interpreted within the framework of the modified model, showing that the presence of mechanical noise can result in a two-slope friction dependence on sliding velocity and also artificially lower the fitted attempt frequency derived from AFM experiments. The model predictions can be verified by experiments when AFM data on friction at high sliding velocity regimes become available.

II. MODEL

Atomic friction is often interpreted using the PT model, where the single asperity of an AFM tip apex is treated as a ball-like tip sliding against a substrate. The tip is dragged by a support displaced at a constant velocity through a harmonic spring (see Fig. 1). The corrugation potential between the tip and substrate is approximated in the sinusoidal form. The total potential energy, which is the sum of the corrugation potential and the elastic potential in the harmonic spring, can
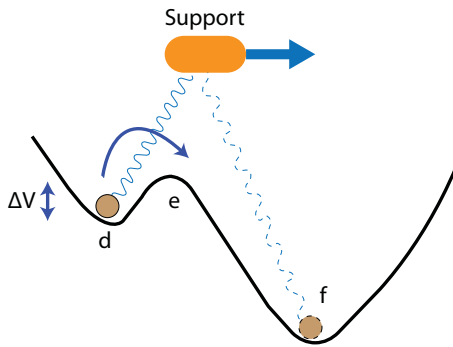

FIG. 1. (Color online) Graphical depiction of the one-dimensional PT model. In this model, an AFM tip having nanoscale dimensions (represented by brown circles) is dragged by a support to slide on an atomically flat and periodic substrate. The total potential energy of the system is represented by the gray curve and evolves with time as the tip slides over the surface. The twisting motion of the cantilever is depicted by the spring attached between the support and the AFM tip. The support provides the scanning motion of the tip along the surface.

be expressed as

$$V(x,t) = -\frac{U}{2}\cos\left(\frac{2\pi x}{a}\right) + \frac{1}{2}k(vt - x)^2, \qquad (2)$$

where x is the position of the tip, t is time, U is the magnitude of the corrugation potential, a is the lattice spacing of the substrate, k is the stiffness of the harmonic spring, and v is the driving speed of the support. At the equilibrium state, the tip will reside in a local minimum d as indicated in Fig. 1. An energy barrier ΔV, the energy difference between the local minimum d and the saddle point e, hinders the tip slipping from d to its adjacent minimum f. Driven by the support, the energy barrier will diminish gradually. In the absence of other sources of energy (thermal or mechanical), slip occurs only when the energy barrier completely vanishes ($\Delta V = 0$), which is when the potential energy stored in the spring is equal to the corrugation potential amplitude. With additional sources of energy, such as thermal and mechanical energy, the tip is able to hop over the energy barrier before the energy landscape at points d and e are equal. Consequently, the lateral force (or friction force) becomes smaller.

Given that almost all atomic friction experiments are conducted at temperatures greater than 0 K, the PT model is typically modified using two different methods to include the effects of thermal energy. One way is to describe the dynamics of the AFM tip using the Langevin equation. The random force resulting from thermal noise can be obtained by the fluctuation-dissipation relation. Although the Langevin equation is useful in accounting for the additional thermal energy, it is difficult to directly include other noise sources that are inherent in AFM instruments.

The second approach is to consider the stochastic nature of noise (thermal and mechanical) present in AFMs using, for example, the Monte Carlo method [29] and master equation method [30]. Indeed, both the Monte Carlo and master equation methods share the same underlying principle and yield similar results. The master equation method is more computationally efficient and statistically reliable than directly solving the Langevin equation, which is used to calculate the displacement, velocity, and acceleration of the tip as a function of time. More specifically, a significant amount of computation time is required to map friction as a function of velocity and temperature when solving the Langevin equation directly, as repetitive calculations would be required for each velocity and temperature data point. Moreover, the application of transition state theory makes it more convenient to incorporate multiple noise sources, allowing one to study velocity dependence of friction in the presence of both instrumental and thermal noise, as opposed to using the Langevin equation as in Ref. [25].

The master equation method stems from statistical mechanics and is suitable for systems where a set of states exists and the occupation of these states is governed by the dynamics of transitions between them [31]. Atomic stick-slip friction falls into this category where the tip may occupy different states (states d and f as shown in Fig. 1), while also under the effect of various noise sources. If we surmise that single stick slip dominates the friction process (which holds true for most experimental observations), the probabilities of the tip

occupying the available states obey the relations below:

$$\frac{dP_d}{dt} = \kappa_{f \to d} P_f - \kappa_{d \to f} P_d,$$
$$\frac{dP_f}{dt} = \kappa_{d \to f} P_d - \kappa_{f \to d} P_f, \tag{3}$$

where $\kappa_{d \to f}$ is the instantaneous transition rate from state d to state f, and vice versa. Both forward and backward transitions are allowed in our calculation. Once the time-dependent probabilities of occupying each state P_d and P_f are determined, physical quantities at any given time can be obtained as weighted averages over all available states.

The key to solving the master equation [Eq. (3)] is to calculate the instantaneous transition rate κ. The transition rate due to thermal activation can be obtained through Arrhenius equation

$$\kappa_t = f_{\text{att}} \exp\left[-\frac{\Delta V}{k_b T}\right], \tag{4}$$

where f_{att} is the attempt frequency associated with thermal activation, ΔV is the energy barrier and is calculated by numerically finding the saddle point (e) and the local minimum (d) as indicated in Fig. 1, k_b is the Boltzmann constant, and T is temperature. The harmonic transition state theory (HTST) can be used to obtain the attempt frequency [19,30]. Based on HTST, the attempt frequency for a transition from local minimum d over saddle point e can be expressed as $f_{\text{att}} = \frac{1}{2\pi} \frac{\Pi_{i=1}^{N} \lambda_i^{(d)}}{\Pi_{j=1}^{N-1} \lambda_j^{(e)}}$, where $\lambda_i^{(d)}$ and $\lambda_j^{(e)}$ are the real vibrational eigenfrequencies at the minimum d and saddle point e, respectively. Then, for a one-spring PT model, assuming no correlated barrier recrossing, the attempt frequency at d can be written as

$$f_{\text{att}} = \frac{w_d}{2\pi}, \tag{5}$$

where $w_d = \sqrt{\frac{V_{xx}(x_d, vt)}{m}}$ is the angular frequency at the local minimum d and m is the effective mass of the tip.

We specifically denote the attempt frequency due to thermal oscillations of the tip as f_{att}, to differentiate this value from the attempt frequency determined in the thermally activated PT model, denoted f_0, as f_0 is the value we are exploring in this paper. Until this point, we have not included the effect of instrumental noise into the master equation. For simplicity, we assume that the instrumental noise takes the form of Gaussian distribution (white noise) at certain characteristic frequencies. In the same way, we can employ the Arrhenius equation [Eq. (4)] to include the influence of instrumental noise in the PT model. For instrumental noise, f_{in} becomes the characteristic frequency of the instrumental noise and the subscript *in* indicates it is for the instrumental noise; T_{eff} is then the effective temperature, which does not have a physical meaning of temperature but rather represents the magnitude of instrumental noise. To explicitly differentiate the effective temperature, which is a scaling factor for the amplitude of the instrumental noise, from real temperature of the system, which yields thermal noise, we will use T_{eff} to denote the scaling factor for the instrumental noise and T for the temperature of the system. Additionally, we assume that T_{eff} is independent of temperature and must be measured for each individual AFM

system. It is also worth pointing out that instrumental noise may come from different sources [26]. By using the master equation method, incorporation of these different noise sources into the thermally activated PT model can be simply achieved. For the moment, we would like to restrict our analysis to one source of noise, which is the noise source with the highest intensity or amplitude.

III. RESULTS

We numerically implement the aforementioned master equation to investigate velocity dependence of atomic friction. A set of parameters are applied such that they are consistent with commonly used values [32]. The magnitude of the corrugation potential $U = 2.0$ eV [in Eq. (2)], the lattice spacing on substrate surface $a = 0.288$ nm, the effective lateral stiffness $k = 1$ N/m, and the mass of the tip apex $m = 10^{-20}$ kg which leads to an attempt frequency for thermal activation f_{att} equal to 1 GHz using Eq. (5). The characteristic frequency for instrumental noise is often on the order of kHz [25]. In our calculation we will vary it from 0.1 to 100 kHz. It is worth emphasizing again that the instrumental noise depends on the individual AFM system. In our calculations, effective temperatures ranging from 0 to 2000 K are used when demonstrating the effect of the variation of the mechanical noise amplitude on thermally activated friction. The mechanical white noise amplitude is considered independent of temperature in all cases, except the final example in this manuscript. This assumption allows us to simplify our calculation and give a qualitative description of the velocity dependence of atomic friction. A quantitatively accurate inclusion of instrumental noise needs specific information from the AFM used in a given experiment [25].

Figure 2 demonstrates velocity and temperature dependence of friction with (a) only thermal noise and (b) both thermal and instrumental noise. Velocities ranging from 1 nm/s to 1 m/s and beyond are included so that the critical friction force F_c can be identified, as well as to link the friction behavior observed at typical sliding speeds used in molecular dynamics simulations of atomic friction and the sliding speeds typically encountered in real mechanical systems with the friction measured at slow sliding velocities typically achieved in AFM experiments. In the case where only thermal noise is considered, friction decreases sublinearly with temperature, increases logarithmically with velocity, and reaches a plateau (transition point) at high velocity regimes, which are consistent with the previous theoretical predictions [4,5]. Once the instrumental noise is introduced, friction at relatively low temperature and low velocity regime is further suppressed [as illustrated in Fig. 2(b)]. The suppression of friction causes the rise of an extra transition point at the low velocity regime. In this work, we will discuss the implication of velocity dependence of atomic friction measured in experiments. Based on the PT model with only thermal activation, the critical velocity at the transition point is proportional to the attempt frequency, $v_c = \frac{2f_0 \beta k_b T}{3 k_{\text{eff}} \sqrt{F_c}}$, where f_0 is the attempt frequency, β is a parameter determined by the shape of the corrugation potential, k_b is the Boltzmann constant, k_{eff} is the effective AFM stiffness, T is temperature, and F_c is the maximum friction at $T = 0$ K. In experiments, the friction plateau
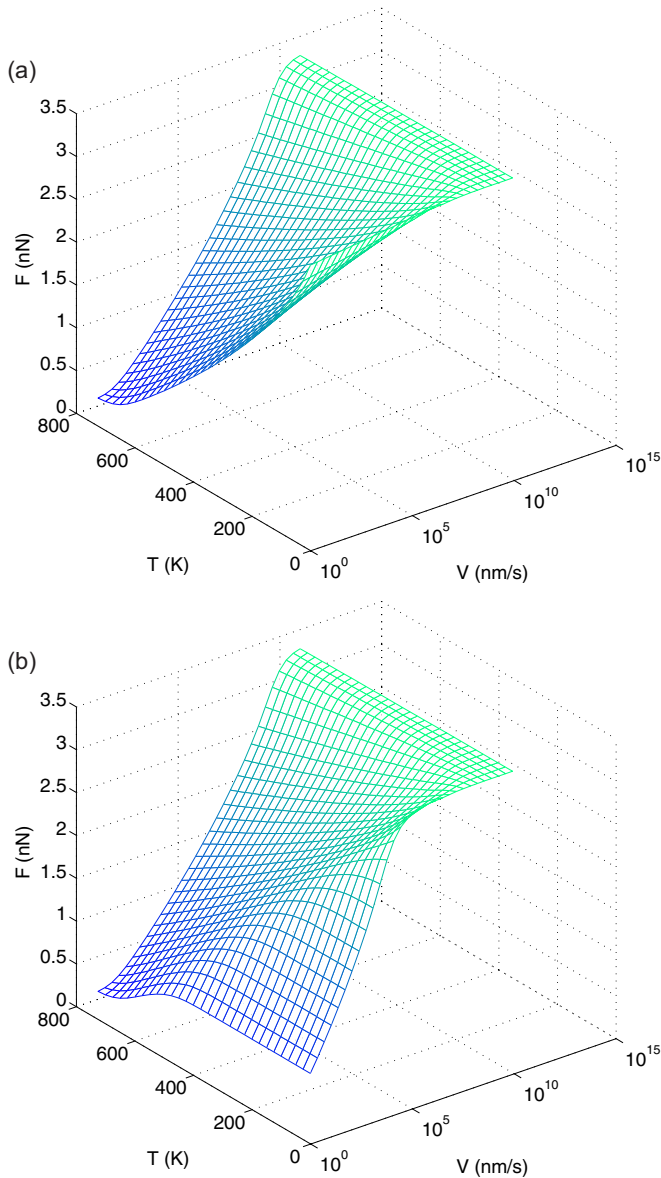
FIG. 2. (Color online) (a) Numerical result showing the variation of the friction force as a function of sliding velocity and temperature when only thermal noise is considered. (b) Numerical result showing the variation of the friction force as a function of velocity and temperature when both thermal noise and instrumental noise are considered. The instrumental noise associated with an effective temperature of $T_{\mathrm{eff}} = 1200$ K at a frequency of $f_{\mathrm{in}} = 10$ kHz is used.

at velocities around μm/s can be obtained [6]. In sharp contrast, this friction plateau usually arises at velocities on the order of m/s in theoretical prediction or molecular dynamics simulation [11,18]. Consequently, the attempt frequencies measured from AFM experiments unanimously fall in the range from kHz to MHz [4–6,9,11], which are much smaller than the theoretical predictions ranging from GHz to THz.

This attempt frequency discrepancy between simulation and experiment can be rationalized by taking instrumental noise into consideration. To examine this further, we focus on the friction versus velocity curves with varying tempera-
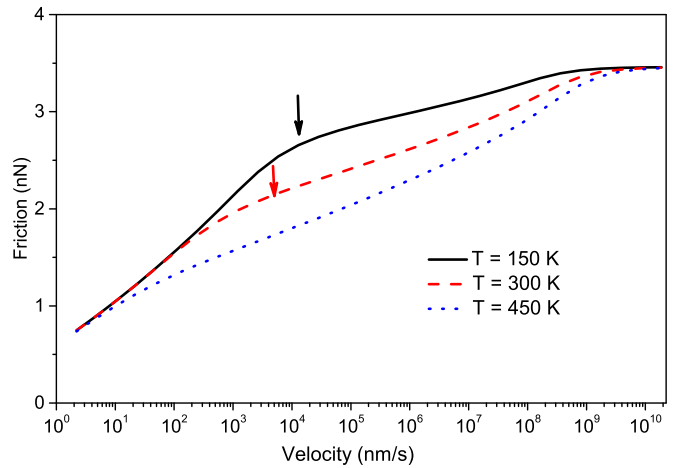

FIG. 3. (Color online) Velocity dependence of atomic friction with both thermal and instrumental noise at different temperatures. Instrumental noise has the parameters $f_{\mathrm{in}} = 10$ kHz and $T_{\mathrm{eff}} = 1200$ K, while the temperature, or the thermal noise, is allowed to vary at a constant attempt frequency. A transition point exists in the friction vs velocity curve as indicated by an arrow, where the dominant friction reducing mechanism transitions from mechanical noise to thermal noise. The attempt frequency for thermal activation (f_{att}) in all cases was 1 GHz.

ture (T), the frequency of the instrumental noise (f_{in}), and the amplitude of the instrumental noise (T_{eff}). Figure 3 shows the velocity dependence of atomic friction at three temperatures. As in the case where instrumental noise is not considered, a friction plateau at high velocity regimes (around 1 m/s) is observed. However, with the addition of instrumental noise, there is now an extra transition point, where the primary friction reducing mechanism transitions from instrumental noise dominated to thermal noise dominated. This point is marked with an arrow in Fig. 3 for $T = 150$ and 300 K and occurs at a very low sliding speed when $T = 450$ K.

The presence of two noise sources results in a two-slope velocity dependence curve where the transition from one slope to the other is marked by this transition point. In the first region, at lower velocities or to the left of the transition point, the instrumental noise gives rise to the dominant slope observed. However, at higher velocities or to the right of the transition point, the second slope results from thermal noise. Given that most AFM measurements are limited to velocities of 1000 nm/s or less, it is likely that the recorded friction versus velocity data are dominated by the influence of instrumental noise, rather than thermal noise and are likely culprits for the very low attempt frequencies reported in the literature.

Closer examination of this transition point shows a general shift toward the lower velocities with increasing temperature. For example, at $T = 150$ K, the transition point occurs at approximately 10 μm/s; at $T = 300$ K, the transition point moves left to a few μm/s; at $T = 450$ K, the transition point is located around 100 nm/s. This gradual decrease in the velocity at which the transition point is observed is a result of thermal noise dominating the reduction of friction at high temperatures, thus eclipsing the influence of instrumental noise on friction. This latter point demonstrates another
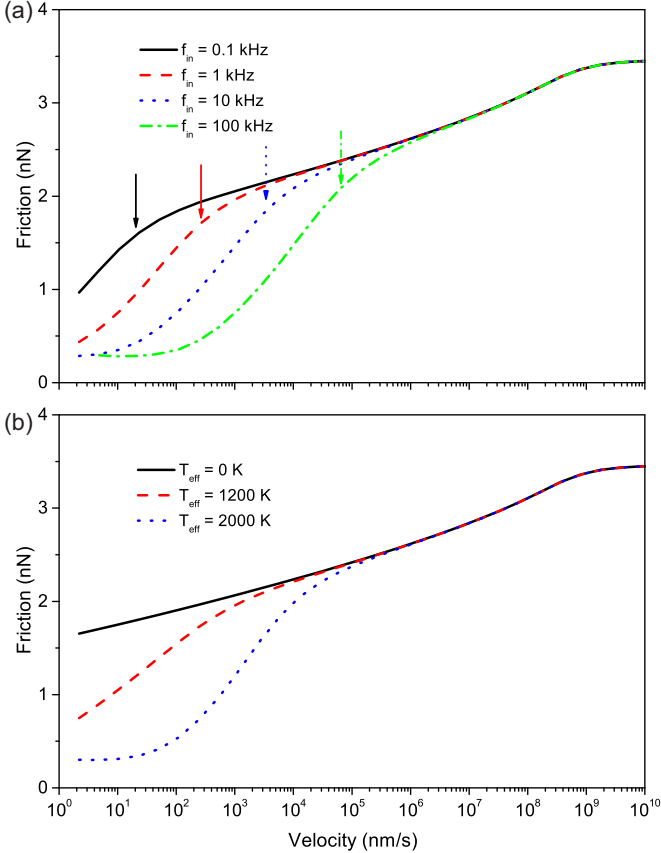
FIG. 4. (Color online) Velocity dependence of atomic friction when both thermal an instrumental noise are accounted for. (a) The frequency of the instrumental noise varied (0.1, 1, 10, and 100 kHz), but a constant $T_{eff} = 2000$ K maintained. Arrows mark the points at which the frequency of the mechanical noise matches the frequency at which the tip traverses the surface atoms. (b) The amplitude of the instrumental noise varied ($T_{eff} = 0$, 1200, and 2000 K), but a constant frequency of 10 kHz maintained. In both (a) and (b), the real temperature (T) is 300 K and the attempt frequency (f_{att}) is 1 GHz.

issue in the experimental literature. There have been a few experimental studies conducted at low temperatures [9,33], compared to even fewer experimental reports of friction at elevated temperatures. The shift of the transition point to lower sliding speeds at high temperatures suggests that a better experimental measurement of the attempt frequency associated with thermal activation, and hence the critical sliding velocity, can only be achieved at friction measurements in the range of 1–1000 nm/s at elevated temperatures, as the influence of instrumental noise is reduced in comparison with thermal noise.

We now examine the influence of the instrumental noise at a constant real temperature. Figure 4(a) shows the influence of the amplitude of the instrumental noise on the measured friction versus velocity trend. Again, the two-slope trend is observed, as in Fig. 3, but the transition point from instrumental to thermal noise dominated behavior shifts to higher frequencies: an increase of one order of magnitude in the instrumental noise moves the transition point to a velocity about one order of magnitude higher. This is because the

transition from instrumental to thermal dominated noise is strongly influenced by the point where the frequency at which the tip traverses the atoms on the surface becomes comparable to the frequency of the mechanical noise. Figure 4(a) also shows that higher frequency noise (beyond 1 kHz) can still have a strong influence on the friction versus velocity trend measured in the <1000-nm/s scanning speed of most experiments.

Second, we examine the influence of changing the amplitude of the instrumental noise at a constant frequency of 10 kHz in Fig. 4(b). A value of $T_{eff} = 0$ K can be interpreted as if the instrumental noise was completely eliminated. As the noise amplitude is increased, we see a decrease in the measured friction at lower sliding speeds, particularly in the range accessible in AFM experiments, but also a gradual shift of the transition point to higher velocities.

IV. DISCUSSION

The results from this theoretical study can aid in the design of appropriate experiments and interpretation of experimental data when fitting measured data to the thermally activated PT model. Specifically, the influences of temperature and instrumental noise amplitude and frequency have been examined using the master equation method, and each is treated independently.

First, if we consider the thermally activated PT model in the absence of instrumental noise, the plateau in the friction versus velocity curve at the critical friction force (F_c) occurs at the critical velocity, defined as $v_c = \frac{2 f_0 \beta k_b T}{3 k_{eff} \sqrt{F_c}}$. Clearly, in the absence of instrumental noise, the critical velocity will increase with temperature. Experimental measurements approaching these velocities may regard the change in slope at the critical velocity as a transition point, which demonstrates a similar change in slope. However, when we include the influence of instrumental noise in the thermally activated PT model, the velocity at which the transition point occurs decreases with increasing temperature, as shown in Fig. 3, in contrast to the critical velocity. Thus, the observation of a decrease in the critical velocity with increasing temperature can be used as an indicator that the friction behavior measured is dominated at low velocities by instrumental noise.

Second, if we examine the influence of the frequency of the instrumental noise on the system, we find that high-frequency noise has a very strong effect on the measured friction behavior at low sliding speeds. Typically, this noise is "eliminated" in most AFM systems with a low pass filter on the friction signal, high oversampling of the friction signals, and scanning in the limited velocity range of 1–1000 nm/s. As specified by Labuda *et al.*, only displacement noise, or noise that can only be measured once the cantilever and sample are in contact, is relevant in velocity-dependent AFM friction measurements [25,26]. Much of the high-frequency noise in AFMs is indeed detection (e.g., from the electronic components of the photodetector) or force (e.g., the thermal vibrations of the cantilever) noise and therefore would not influence the friction behavior. On the other hand, the mechanical resonance of the piezo is typically on the order of kHz and could be a source of "high-frequency" displacement noise. Despite these efforts to reduce all noise sources and achieve lattice resolution

images, the velocity-dependent friction behavior will not reflect the thermal activation of friction described in the thermally activated PT model. However, most AFM experimentalists spend a significant amount of effort to eliminate low-frequency vibrations, or those less than 1 kHz. Figure 4 shows that a transition point will likely be identifiable in the range of scanning velocities that is accessible to most experimentalists if low-frequency noise dominates all other sources of instrumental noise and should not be mistaken for the critical velocity expected from thermal activation.

Two other conclusions can be drawn from the data shown in this paper: experimentalists are advised to examine the thermal activation of friction at elevated temperatures, rather than low temperatures; and experimentalists should increase the velocity at which they can achieve friction measurements. By studying atomic friction at higher temperatures, the thermal activation of friction dominates the instrumental noise at increasingly lower scanning speeds. In fact, at temperatures of just 450 K (or 177 °C—a temperature easily reached in most UHV if not ambient systems) Fig. 3 shows that thermal activation of friction can be directly studied at sliding speeds already accessible in most AFM systems. On the other hand, low temperature measurements reduce the influence of thermal activation on atomic friction measurements and increase the influence of instrumental noise. In addition, higher speed experimental measurements, whereby velocities of mm/s could be achieved, would be ideal. At high velocity regimes, the transition point can be overcome and experimental verification of the two-slope variation in the friction versus velocity behavior could likely be confirmed. Furthermore, comparison with advanced simulation techniques, such as parallel replica dynamics [34], can be achieved, allowing for a verification of the thermally activated model of friction.

Finally, the objective of this paper is to show that, through the introduction of instrumental noise, artificially low attempt frequencies (f_0) would be obtained from fitting the thermally activated PT model to velocity-dependent friction data, which is often acquired at velocities less than 1000 nm/s. Table I verifies the supposition, first suggested by Riedo *et al.* [6], that mechanical noise is responsible for lowering the thermally

TABLE I. Values of attempt frequencies (f_0) determined from the figures within this paper determined using the thermally activated PT model in velocity ranges of 1–1000 nm/s. The color column refers to the color and line type of the line in each of the figures.

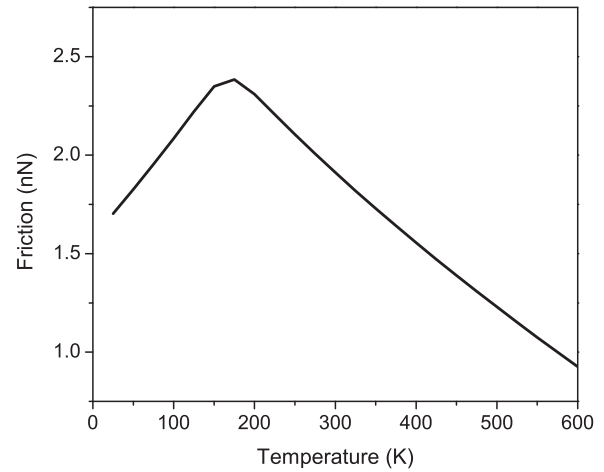| Figure number	Line color		Attempt frequency f_0 (kHz)
3	Black	(Solid)	0.8
	Red	(Dashed)	1.0
	Blue	(Dotted)	1.4
4(a)	Black	(Solid)	0.03
	Red	(Dashed)	0.2
	Blue	(Dotted)	2.0
4(b)	Black	(Solid)	10^6
	Red	(Dashed)	1.0
	Blue	(Dotted)	2.0

FIG. 5. Variation of friction with temperature in the presence of instrumental noise whose amplitude depends on the sample temperature. The instrumental noise has a frequency (f_{in}) of 10 kHz, $f_{att} = 1$ GHz, and the amplitude varies such that at $T > 300$ K, $T_{eff} = 0$ K and for $T < 300$ K, $T_{eff} = 4(300 - T)$. Other parameters used in this thermally activated PT model are the same as in the other graphs.

activated attempt frequency downward to kHz. To demonstrate this, we have fit the data shown within this paper, assuming no instrumental noise and in the 1–1000 nm/s velocity range using the thermally activated Tomlinson model, calculating the attempt frequency from the fit parameters. The values are summarized in Table I. The measured attempt frequencies are in the range of 0.5–2 kHz, closer to what is often reported in experimental studies [6,11], despite the frequency of the tip apex due to thermal energy being constant at $f_{att} = 1$ GHz in our models. Therefore, to rectify the gap in reported attempt frequencies determined using the thermally activated model, experimentalists are advised to better characterize the instrumental displacement noise in their microscopes, and those conducting simulations should attempt to include these effects in their calculations.

Before concluding this study, we examine an interesting trend in the friction versus temperature behavior that has been experimentally measured and modeled [35,36]. In these studies, friction was studied from temperatures around 100 K to room temperature. A gradual increase in friction was observed from 100 K until a maximum was observed at 125–225 K depending on the experiment, followed by decreasing friction until room temperature was reached. We propose an alternate model to explain this observed trend. Figure 5 reproduces this complex friction versus temperature dependence by varying T_{eff} with temperature. Given the strong mechanical coupling of the cooling apparatus (likely a flow cryostat) with the sample itself, it is not unreasonable to assume that an increase in displacement or instrumental noise would be observed when cooling a sample. However, given that there have been no published measurements of the instrumental noise associated with cooling a sample in an AFM, and how that instrumental noise varies with the cooling output of the cryostat, we cannot be certain that the amount of instrumental noise at the sample-tip contact would change with sample temperature.

We therefore present this idea as an alternative to the proposed model by Barel and colleagues to explain their friction results. However, its validation requires experimental evaluation of the noise level of the cooling system imposed on the AFM measurements.

V. CONCLUSION

In summary, it has been shown that the inclusion of instrumental noise in atomic friction measurements of velocity-dependent friction is substantial. Furthermore, the experimentally observed logarithmic relation between velocity and atomic friction, particularly at the slow scanning speeds reported in experimental measurements, results from the mutual contributions of both thermal and instrumental noise. The low attempt frequency and the resultant low critical velocity measured in AFM experiments primarily result from the instrumental noise inherent in AFM measurements. This result indicates that extreme caution is needed when interpreting experimental AFM data of friction versus velocity or temperature. Our model also provides clues for experimentalists on key parameters that would aid in verifying the existence and significance of the instrumental noise inherent in AFM measurements. Specifically, a decrease of the transition point with temperature and the appearance of a two-slope curve of the friction versus velocity data would suggest the presence of significant instrumental noise influencing the measurement. The predictions invite further experimental investigations under higher sliding velocities [37] and higher temperatures to reduce the influence of inherent instrumental noise in their experimental measurements. Finally, a temperature-dependent mechanical noise has been introduced into the thermally activated PT model, which reproduces an unusual temperature dependence of atomic friction that has been experimentally measured.

[1] G. Binnig, C. F. Quate, and C. Gerber, Phys. Rev. Lett. **56**, 930 (1986).

[2] C. M. Mate, G. M. McClelland, R. Erlandsson, and S. Chiang, Phys. Rev. Lett. **59**, 1942 (1987).

[3] R. Bennewitz, T. Gyalog, M. Guggisberg, M. Bammerlin, E. Meyer, and H. J. Güntherodt, Phys. Rev. B **60**, R11301 (1999).

[4] E. Gnecco, R. Bennewitz, T. Gyalog, C. Loppacher, M. Bammerlin, E. Meyer, and H. J. Güntherodt, Phys. Rev. Lett. **84**, 1172 (2000).

[5] Y. Sang, M. Dubé, and M. Grant, Phys. Rev. Lett. **87**, 174301 (2001).

[6] E. Riedo, E. Gnecco, R. Bennewitz, E. Meyer, and H. Brune, Phys. Rev. Lett. **91**, 084502 (2003).

[7] B. Persson, O. Albohr, F. Mancosu, V. Peveri, V. Samoilov, and I. Sivebæk, Wear **254**, 835 (2003).

[8] M. Brukman, G. Gao, R. Nemanich, and J. Harrison, J. Phys. Chem. C **112**, 9358 (2008).

[9] L. Jansen, H. Hölscher, H. Fuchs, and A. Schirmeisen, Phys. Rev. Lett. **104**, 256101 (2010).

[10] C. Greiner, J. Felts, Z. Dai, W. King, and R. W. Carpick, Nano Lett. **10**, 4640 (2010).

[11] Q. Li, Y. Dong, D. Perez, A. Martini, and R. W. Carpick, Phys. Rev. Lett. **106**, 126101 (2011).

[12] Y. Dong, Q. Li, and A. Martini, J. Vac. Sci. Technol. A **31**, 030801 (2013).

[13] P. Reimann and M. Evstigneev, New J. Phys. **7**, 25 (2005).

[14] D. G. Abel, S. Y. Krylov, and J. W. M. Frenken, Phys. Rev. Lett. **99**, 166102 (2007).

[15] Z. Tshiprut, A. Filippov, and M. Urbakh, J. Phys. Condens. Matter **20**, 354002 (2008).

[16] S. Krylov and J. Frenken, J. Phys.: Condens. Matter **20**, 354003 (2008).

[17] K. B. Jinesh, S. Y. Krylov, H. Valk, M. Dienwiebel, and J. W. M. Frenken, Phys. Rev. B **78**, 155440 (2008).

[18] D. Perez, Y. Dong, A. Martini, and A. F. Voter, Phys. Rev. B **81**, 245415 (2010).

[19] Y. Dong, H. Gao, and A. Martini, Europhys. Lett. **98**, 16002 (2012).

[20] Y. J. Song, A. F. Otte, V. Shvarts, Z. Zhao, Y. Kuk, S. R. Blankenship, A. Band, F. M. Hess, and J. A. Stroscio, Rev. Sci. Instrum. **81**, 121101 (2010).

[21] J. B. Thompson, B. Drake, J. H. Kindt, J. Hoskins, and P. K. Hansma, Nanotechnology **12**, 394 (2001).

[22] E. Gnecco, A. Socoliuc, S. Maier, J. Gessler, T. Glatzel, A. Baratoff, and E. Meyer, Nanotechnology **20**, 025501 (2009).

[23] M. A. Lantz, D. Wiesmann, and B. Gotsmann, Nature Nanotechnology **4**, 586 (2009).

[24] A. Socoliuc, E. Gnecco, S. Maier, O. Pfeiffer, A. Baratoff, R. Bennewitz, and E. Meyer, Science **313**, 207 (2006).

[25] A. Labuda, M. Lysy, W. Paul, Y. Miyahara, P. Grütter, R. Bennewitz, and M. Sutton, Phys. Rev. E **86**, 031104 (2012).

[26] A. Labuda, J. Bates, and P. Grütter, Nanotechnology **23**, 025503 (2011).

[27] G. Tomlinson, Philos. Mag. **7**, 905 (1929).

[28] L. Prandtl, Z. Angew. Math. Mech. **8**, 85 (1928).

[29] O. J. Furlong, S. J. Manzi, V. D. Pereyra, V. Bustos, and W. T. Tysoe, Phys. Rev. B **80**, 153408 (2009).

[30] Y. Dong, D. Perez, H. Gao, and A. Martini, J. Phys. Condens. Matter **24**, 265001 (2012).

[31] R. Zwanzig, *Nonequilibrium Statistical Mechanics* (Oxford University, New York, 2001).

[32] Y. Dong, A. Vadakkepatt, and A. Martini, Tribol. Lett. **44**, 367 (2011).

[33] A. Schirmeisen, L. Jansen, H. Hölscher, and H. Fuchs, Appl. Phys. Lett. **88**, 123108 (2006).

[34] A. Martini, Y. Dong, D. Perez, and A. F. Voter, Tribol. Lett. **36**, 63 (2009).

[35] I. Barel, M. Urbakh, L. Jansen, and A. Schirmeisen, Phys. Rev. B **84**, 115417 (2011).

[36] I. Barel, M. Urbakh, L. Jansen, and A. Schirmeisen, Tribol. Lett. **39**, 311 (2010).

[37] N. S. Tambe and B. Bhushan, Nanotechnology **16**, 2309 (2005).